The Contribution of NMDA Receptors to Contrast Coding in ON Retinal Ganglion Cells of *Mus musculus*

By

Tamatea Westby

A Thesis Submitted in Partial Fulfillment of the
Requirements of the Degree of

BACHELOR OF SCIENCE HONOURS

In the Department for Biology

University of Victoria

The Contribution of NMDA Receptors to Contrast Coding in ON Retinal Ganglion Cells of *Mus musculus*

By

Tamatea Westby

Supervisory Committee
Dr. Gautam Awatramani, Supervisor
Department of Biology

Abstract

The retina encodes contrast (the difference in light intensity between an object and its background) using a complex network of neurons that end in ganglion cells (GCs) which transmit visual signals to the brain. GCs express both AMPA and NMDA-type glutamate receptors, with NMDA receptors (NMDARs) having high glutamate affinity and variable localization patterns. Previous studies in guinea pig retinas found no NMDAR contribution to contrast coding in ON-∝ GCs but found that these receptors were expressed in mice ON-GCs. My study investigated the contribution of NMDARs to contrast coding in mouse ON-GCs. I used whole-cell voltage clamp electrophysiology in ON-GCs from *Mus musculus* retinas and recorded light-evoked responses to spots of varying contrast. I then determined receptor-specific contributions to the recorded responses using a deconvolution technique which avoided the potential confounding effects of using pharmacology. I first investigated whether NMDARs contribute to low contrast responses and then examined how their conductance changes with increasing contrast. The results revealed a significant NMDAR component to low contrast responses that scaled with increasing contrast. These findings provide new insight into contrast coding mechanisms in the retina, suggesting that NMDARs play a key role in shaping ON-GC responses.

Table of Contents

Table of Figures

Acknowledgements

I would like to thank Dr. Gautam Awatramani for this opportunity and for graciously mentoring me throughout the process. I would also like to thank the rest of the Awatramani lab for their guidance in experimental and analytical techniques. I especially acknowledge Ilya Capralov for his patience in training and teaching me. Lastly, I would like to thank my mom and dad for their support throughout this project.

Chapter 1: Introduction

1.1 The Retina

The retina is a complex sensory structure located at the back of the eye that is responsible for encoding and processing visual information. It is composed of millions of neurons across more than 60 distinct cell types (Masland, 2012). Visual processing begins with phototransduction (the conversion of photons into electrical signals) by photoreceptors (PRs), which then release glutamate: the retina's primary excitatory neurotransmitter (Molday & Moritz, 2015; Connaughton, 1995). This glutamate activates bipolar cells (BPCs), which are functionally divided into ON and OFF types (Ichinose & Habib, 2022). ON-BPCs depolarize in response to increases in illumination, while OFF-BPCs depolarize in response to decreases (Ichinose & Habib, 2022). BPCs subsequently release glutamate onto both amacrine cells (ACs) and ganglion cells (GCs) (Miller, 2008). ACs are interneurons with diverse roles in visual processing, whereas GCs are the retina's primary output neurons that send highly processed information to the brain (Macneil & Masland, 1998; Masland, 2012). More than 30 types of GCs have been identified that are each sensitive to distinct visual features (Sanes & Masland, 2015). In summary, the retina encodes visual information through an intricate network of specialized neurons, with GCs transmitting the final processed signals to the brain.

1.2 Contrast Coding

Among the many visual features encoded by GCs is contrast, which is the difference in light intensity between an object and its background. Contrast coding is essential for distinguishing objects within a dynamic visual environment. Ambient light levels within the visual environment can vary more than nine orders of magnitude, however, sensory neurons have a limited dynamic range (Smirnakis et al., 1997; Yedutenko et al., 2021). One way this limitation is mitigated is through encoding contrast, which allows for relative comparisons against a baseline. As a result, the visual system can represent a broad range of light intensities while preserving subtle

variations (Yedutenko et al., 2021). Therefore, contrast coding in GCs is a critical aspect of vision, allowing the interpretation of complex visual scenes across a wide range of lighting conditions.

1.3 GC Glutamate Receptors

Glutamate receptors play an essential role in detecting and encoding the signals that GCs receive. GCs primarily express two main types of ionotropic glutamate receptors (AMPA and NMDA), which both have unique characteristics (Miller, 2008). Firstly, these receptors differ in their biophysical properties. AMPA receptors (AMPARs) have a linear current-voltage relationship, meaning that the flow of electrical charges through the channel changes linearly with change in membrane potential (the difference in electrical charge between the inside and the outside of the neuron) (Dingledine et al., 1999). In contrast, NMDA receptors (NMDARs) have a J-shaped current-voltage relationship, due to a magnesium ion blocking the channel which requires depolarization to be removed (Dingledine et al., 1999; Nowak et al., 1984; Traynelis, et al., 2010). Another distinction between these receptors is their affinity for glutamate, which is quantified by their EC_{50} values (the glutamate concentration required to evoke a half-maximal response) which are approximately 2.3 μM for NMDARs and 480 μM for AMPARs (Patneau & Mayer, 1990; Traynelis et al., 2010). Lastly, these two receptors have been shown to differ in their localization patterns in GCs. AMPARs are mainly localized within the synapse (synaptically), whereas NMDARS can be localized synaptically or outside of the synapse (extrasynaptically) (Chen & Diamond, 2002; Kalbaugh et al., 2009; Sagdullaev et al., 2006; Zhang & Diamond, 2009). In summary, there are two main types of glutamate receptors expressed by GCs which are both unique in their functionality and their localization.

1.4 Retinal Signal Transmission

The signals that GC glutamate receptors receive are complex and span a broad range of frequencies. Most of the cells in the retina communicate through graded potentials, enabling continuous and precise encoding of visual information (Baylor & Fuortes, 1970; Juusola & French, 1997; Kaneko, 1970). To effectively transmit these

signals between cells, the retina uses ribbon synapses, which are specialized structures that allow for rapid and sustained multivesicular glutamate release, thereby broadening the range of signal transmission (Singer, 2007). However, once the signals reach GCs, they are converted into action potentials to enable long distance transmission to the brain (Berry et al., 1997; Purves et al., 2001). This transition from graded synaptic input to spiking output presents a challenge for GC glutamate receptors, which must encode and preserve the broad range of complex signals from presynaptic neurons.

1.5 GC NMDARs and Contrast Coding

The high glutamate affinity and distinct localization patterns of NMDARs in GCs could allow for a unique contribution to encoding broad-range complex signals like contrast (Figure 1). NMDARs localized synaptically could contribute at low contrast by detecting small amounts of glutamate release due to their high affinity (Manookin et al., 2010; Zhang & Diamond, 2009). Alternatively, extrasynaptically localized NMDARs could contribute at high contrast by detecting glutamate spillover from the synapse (Chen & Diamond, 2002; Manookin et al., 2010). However, the contribution of NMDARs to contrast coding is not well understood.

Manookin et al., (2010) investigated the contribution of NMDARs to contrast coding in guinea pig GCs. They used electrophysiology to record GC responses to stimuli of varying contrasts and applied a novel deconvolution method to determine receptor-specific contributions to these responses: a process typically achieved by pharmacologically isolating components through receptor antagonism. This deconvolution method was used to avoid potential non-specific effects of pharmacology acting on upstream retinal circuitry (Kalbaugh et al., 2009; Sagdullaev et al., 2006). They found that in ON-∝ GCs (a specific type of ON-GCs) there was no NMDAR contribution at any contrast. However, they also found that NMDARs were present in ON-∝ GCs and other ON-GC types in mice but did not investigate their functional contribution. These findings leave a clear research gap to investigate the role of NMDARs in contrast coding in mice ON-GCs.

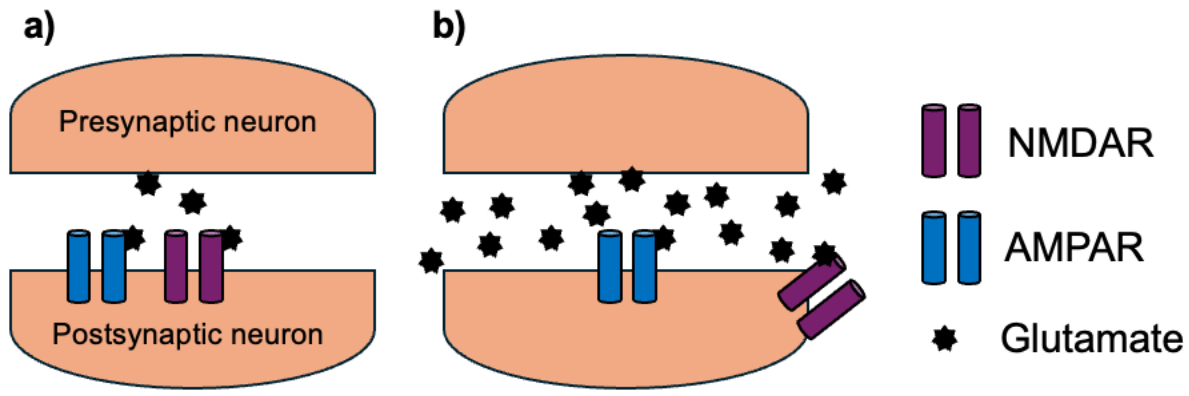

Figure 1. A schematic depicting how different localization of NMDAR could contribute to encoding high and contrast in retinal GCs

(a) Demonstrates a low contrast scenario where there is minimal glutamate release. NMDARs located at the synapse could help detect this glutamate due to their high affinity. (b) A high contrast scenario where there is high glutamate release which can spill out of the synapse. High affinity extrasynaptically localized NMDARs could help encode this spillover.

1.6 Research objectives and Results

My research will investigate the contribution of NMDARs to contrast coding in mouse retinal ON-GCs. I will use electrophysiology in combination with a similar deconvolution method to Manookin et al., (2010) to avoid non-specific effects of pharmacology. This research is novel because it focuses on ON-GCs in mice, investigates NMDAR contribution to light-evoked responses, and does so without the use of pharmacology. The specific objectives will be to address if NMDARs contribute to low contrast responses and how NMDAR contribution changes across contrast levels. The results demonstrated that NMDARs contribute significantly to low contrast responses. Additionally, NMDARs contribute across all contrasts and scaled in magnitude with increasing contrast. These findings extend our understanding of contrast coding, as well as how NMDARs can be utilized within the retina.

Chapter 2: Methods and Materials

2.1 Animals

I experimented on wild-type *Mus musculus* of both sexes between the ages of 2 and 6 months. The animals were group housed with a 12-hour light/dark cycle. I performed all procedures in accordance with the Canadian Council on Animal Care under approval by the University of Victoria's Animal Care Committee.

2.2 Retina Preparation

I first placed the mice in the dark for 45 minutes to allow for the dark adaptation of the retinas to optimize light-evoked responses during experimentation. During this period, I prepared Ringer's solution (Appendix 1), heated it to 35°C, and bubbled it with carbogen gas (95% O_2, 5% CO_2). Additionally, I set up the perfusion chamber by cutting a 2 mm diameter circular hole in 0.22 mm membrane filter paper and adhering it within the chamber (Figure 2a).

After the adaptation period, I euthanized the mice using isoflurane followed by cervical dislocation. Next, I removed both eyes and placed them in a petri dish of Ringer's solution, which was continuously bubbled with carbogen gas. Then, I removed the retina from one of the eyes using an infrared dissecting microscope. I set the other eye aside as a backup in case the first preparation was inadequate.

The process of retina removal involved making a circumferential cut around the cornea, removing the lens, tearing away the sclera and choroid layers, trimming the optic nerve, and clearing away the vitreous humour. After removal, I made an incision in the retina two-thirds of the way to the optic disc to allow it to flatten. Then, I filled the pre-prepared perfusion chamber with Ringer's solution and mounted the retina (ganglion side up) to the filter paper over the pre-cut window (Figure 2b).

Next, I visualized the retina under infrared light using an Olympus BX51WI upright microscope with a 60x water-immersion objective (Figure 3), a Teledyne Retiga ELECTRO CCD camera, and the image acquisition software OCULAR by Teledyne.

Finally, I created a window in the inner limiting membrane using a sharp, high-resistance micropipette to allow access to the GC layer (Figure 2c).

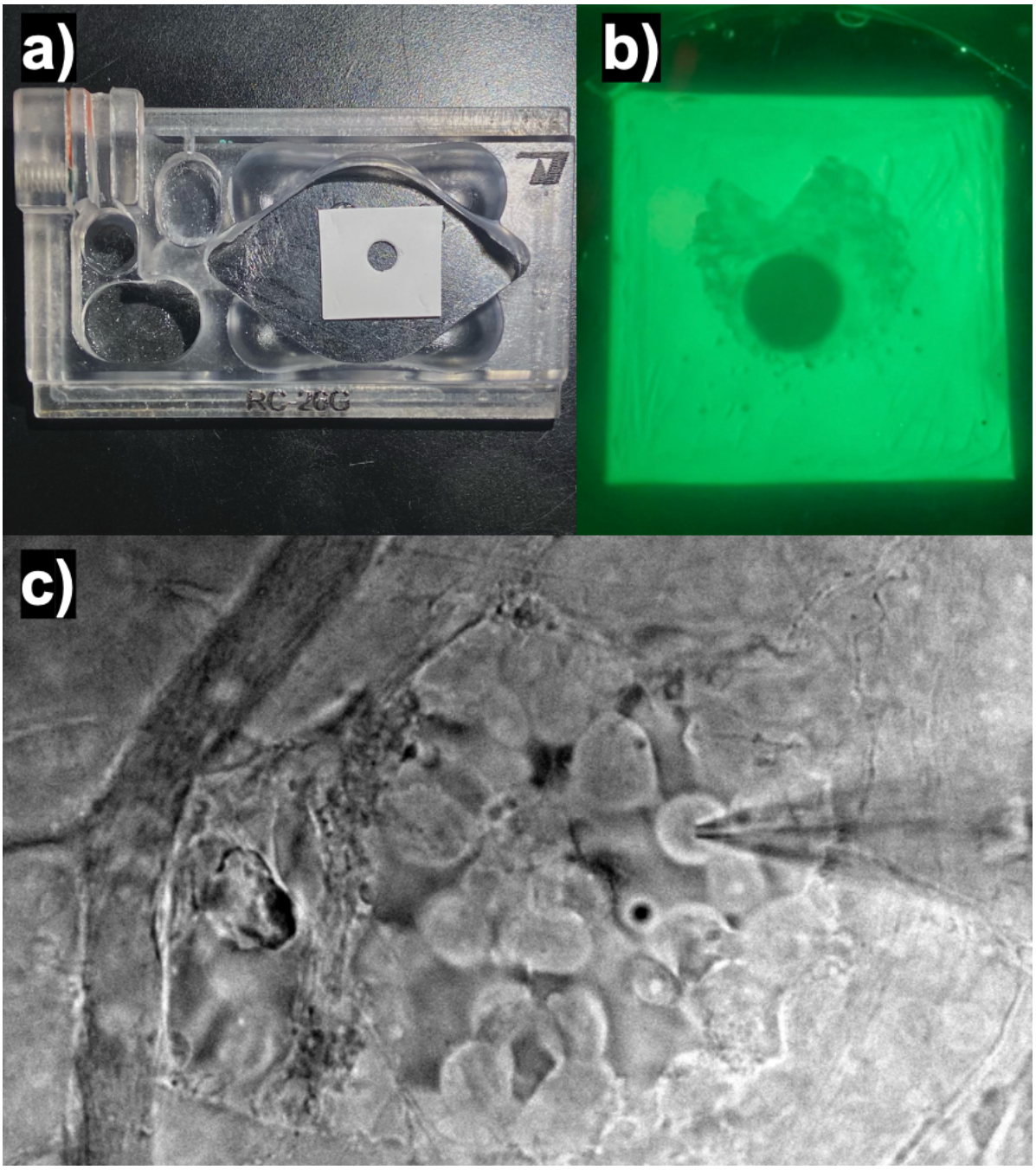

Figure 2. Preparation for electrophysiology

(a) The perfusion chamber with membrane filter paper adhered to it. (b) A retina mounted on the filter paper over the window that allows for stimulus presentation. (c) A window in the inner limiting membrane of the retina with a micropipette patched onto a cell.

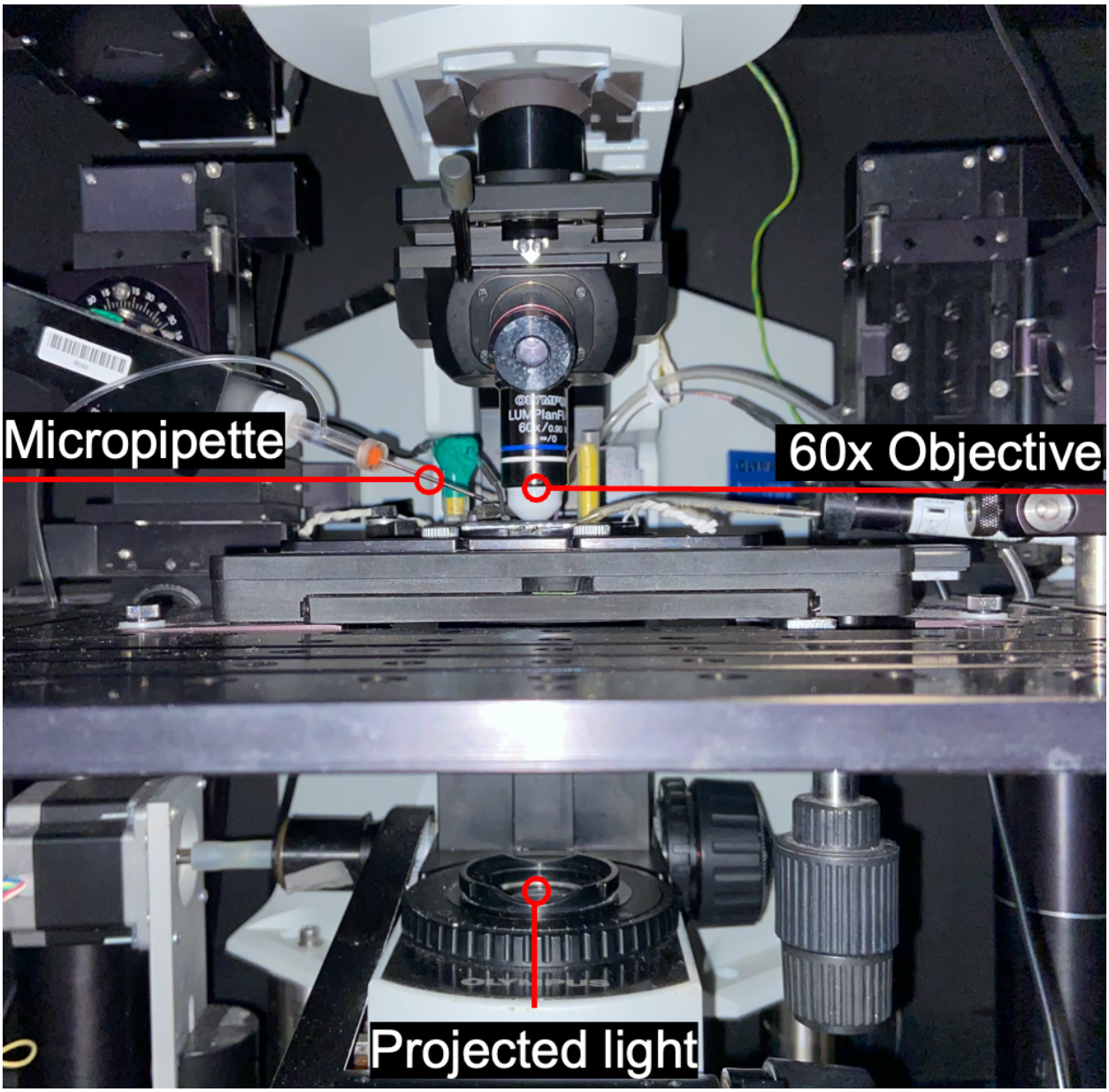

Figure 3. The experimental setup

An annotated photo of the setup for visualizing the retina and conducting electrophysiology. The light is projected through the condenser at the bottom. A 60x water immersion objective is used to visualize the retina. A glass micropipette with a microelectrode within is used for electrophysiology.

2.3 Visual Stimulation

An Epson EX5210 projector was used to produce the light for the experiment. I designed and presented the stimulus for the experiment using Stimgen (Designed by

Ben Murphy-Baum) in MATLAB developed by Mathworks. I used a spot of 200 μm diameter at high contrast for identifying cells with loose patch electrophysiology. For the voltage-clamp electrophysiology, I used three 200 μm diameter spots with increasing contrast: low contrast was high enough to evoke a response but remained below the threshold of inhibition, high contrast was full intensity, and mid contrast was set in between these levels. I centred the stimuli over the soma of the GCs and focused the stimuli on the PR layers using the sub-stage condenser.

2.4 Electrophysiology

I amplified the recordings using Molecular Devices MultiClamp 700B and digitized them at 10kHz with a Molecular Devices Digidata 1550B. For software, I used Molecular Devices MultiClamp as a command program and Molecular Device pCLAMP for data acquisition. I calculated the latency between the onset of the stimuli and the responses in the electrophysiological recordings to be approximately 0.1 seconds.

I began by identifying ON-GCs based on their response to the presentation of the stimuli during loose patch recordings (Figure 4). For these recordings, I used 3-8 megaohm resistance micropipettes filled with Ringer's solution. After I identified the GCs, I proceeded to whole-cell patch them to allow for the voltage-clamping. I used 3-8 megaohm resistance micropipettes filled with Internal solution (Appendix 2) for the whole cell patching. I first held the cells at -60mv, before initiating the experiment: this consisted of voltage steps (first stepping to -70mv, and then up in 20mv increments until reaching +50mV), concurrently with light stimulus presentation at each step (Figure 5). Additionally, I did a 10mv voltage step at the start of each recording to allow assessment of the access resistance. I conducted four trials of the experiment for each cell.

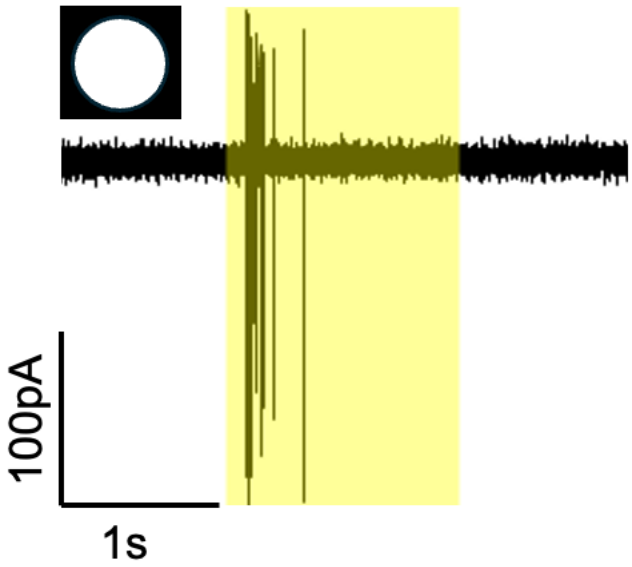

Figure 4. A loose-patch electrophysiological recording demonstrating an ON-response in a mouse retina GC.

The stimulus (top left) was presented during the period indicated by the yellow shading. The black line and spike (action potentials) are the electrophysiological recording. Spiking at the onset of light indicates an ON response. The vertical scale-bar is current (100 pA), and the horizontal scale bar is time (1 second).

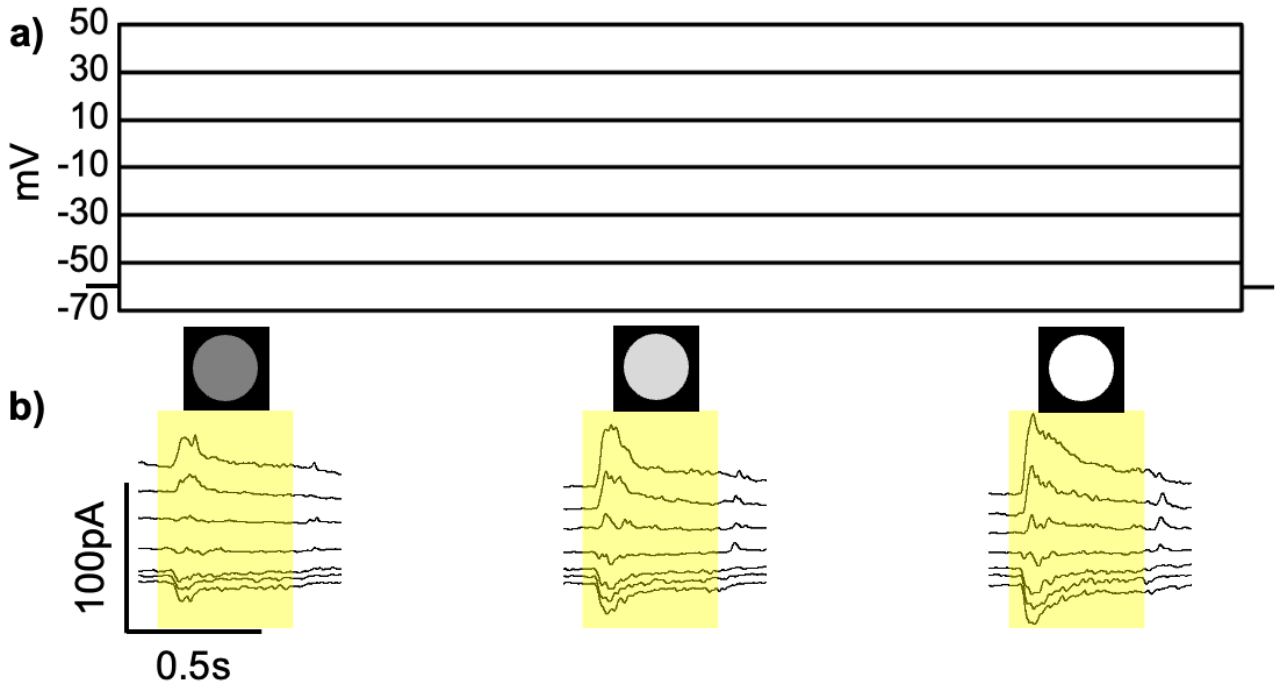

Figure 5. A schematic of the voltage-clamp electrophysiological experiment used to determine the contrast-dependent responses in a mouse retina ON-GC.

(a) A graph of the voltage-step protocol used: the membrane potential was initially held at -60mV, then stepped down to -70mV, and subsequently depolarized in increments of +20mV up to +50mV. (b, top) shows the stimuli that were presented, from low contrast to high contrast. (b, bottom) shows the electrophysiological recording (current responses) corresponding to the duration of stimulus presentation (yellow shading). The vertical scale bar represents current (100 pA), horizontal scale bar indicates time (0.5 seconds)

2.5 Analysis

I analyzed the data using Neurotools (Designed by Ben Murphy-Baum) and Igor from Wavemetrics and performed statistical analysis and graphing using Microsoft Excel and GraphPad Prism. I only included recordings in my data sets if the holding current was $\leq 200pA$, and the access resistance was low (approximated from the test pulse at the beginning of each recording). I chose these parameters to ensure undesirable recordings were not included. Additionally, some of my recordings had a minor offset issue; this was accounted for by shifting the x-axis (a maximum of 10mv).

To begin the analysis, I first processed the raw data into current-voltage relationships on a cell-by-cell basis. I used a 50Hz low pass filter on the data to reduce noise. Then, for each contrast individually, I calculated the relative time-averaged

current value at each given voltage (Appendix 3). I plotted these values to visualize the current-voltage relationship. Afterwards, I averaged across four trials to produce average current-voltage relationships and calculated the standard error of the mean (SEM) for each point.

Next, I determined the receptor-specific contribution to the current-voltage relationship. I fitted a function (Appendix 4) to the averaged experimental data, which provided a weighted sum of the contributing receptor basis functions (their characteristic current-voltage relationship) (Figure 6). To compare, I performed an additional fit excluding NMDAR conductance (Figure 7 a/b top). I also calculated the variance between each fit and the averaged experimental data (Figure 7 a/b bottom). Following this, I calculated the root mean squared error and standard error (SE) of each of the variances to allow for a direct comparison of the fits (Figure 7 c). Through this process, I identified the best fit, which was then used to quantify the contribution of each receptor's conductance at each contrast. I repeated this fitting process across all contrast and cells.

Subsequently, I computed summary statistics of the data. I categorized data into a low-contrast data set (n = 6) and a changing-contrast data set (n = 3). For the low-contrast data set, I calculated the relative conductance of NMDAR and AMPAR by dividing each by the total conductance. I also calculated the mean and SEM. I plotted the relative conductance for each cell as a grouped scatter plot, including means and SEM. For the changing-contrast data set, I calculated the mean and SEM of receptor conductances at each contrast and visualized these data using a line graph.

Finally, I performed statistical analysis, with all tests using a significance level of $\propto = 0.05$. I first assessed normality using a Shapiro-Wilk test. For the low-contrast data set, I used a Wilcoxon signed-rank test to determine whether the median NMDAR conductance was significantly greater than zero. For the changing-contrast data set, I conducted a one-tailed, one-sample t-test at each contrast to test if the mean NMDAR conductance was significantly greater than zero. Then, I conducted a one-tailed, paired-sample t-test to test whether NMDAR conductance increased with contrast.

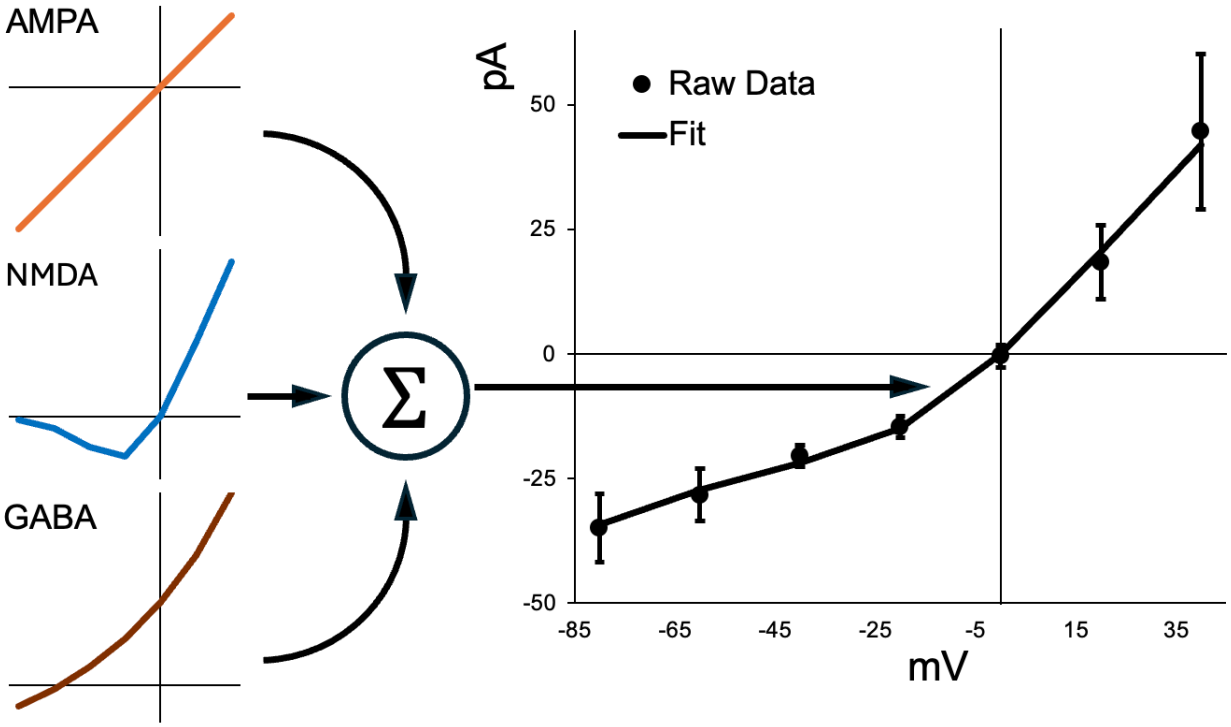

Figure 6. An illustration of the fitting process used to determine the receptor-specific contribution (AMPAR, NMDAR, and GABAR) to the current-voltage relationship of light-evoked responses measured with voltage-clamp electrophysiology from a retinal ON-GC in mice.

The left graphs depict individual basis functions for the current-voltage curves of AMPAR (orange), NMDAR (blue) and GABAR (brown). The basis functions are weighted and summed to produce a best-fit curve for the experimentally measured data. The right graph represents the four-trial averaged experimental data (black dots), with error bars indicating SEM and the black line shows the resulting fit obtained from summing the receptor contributions.

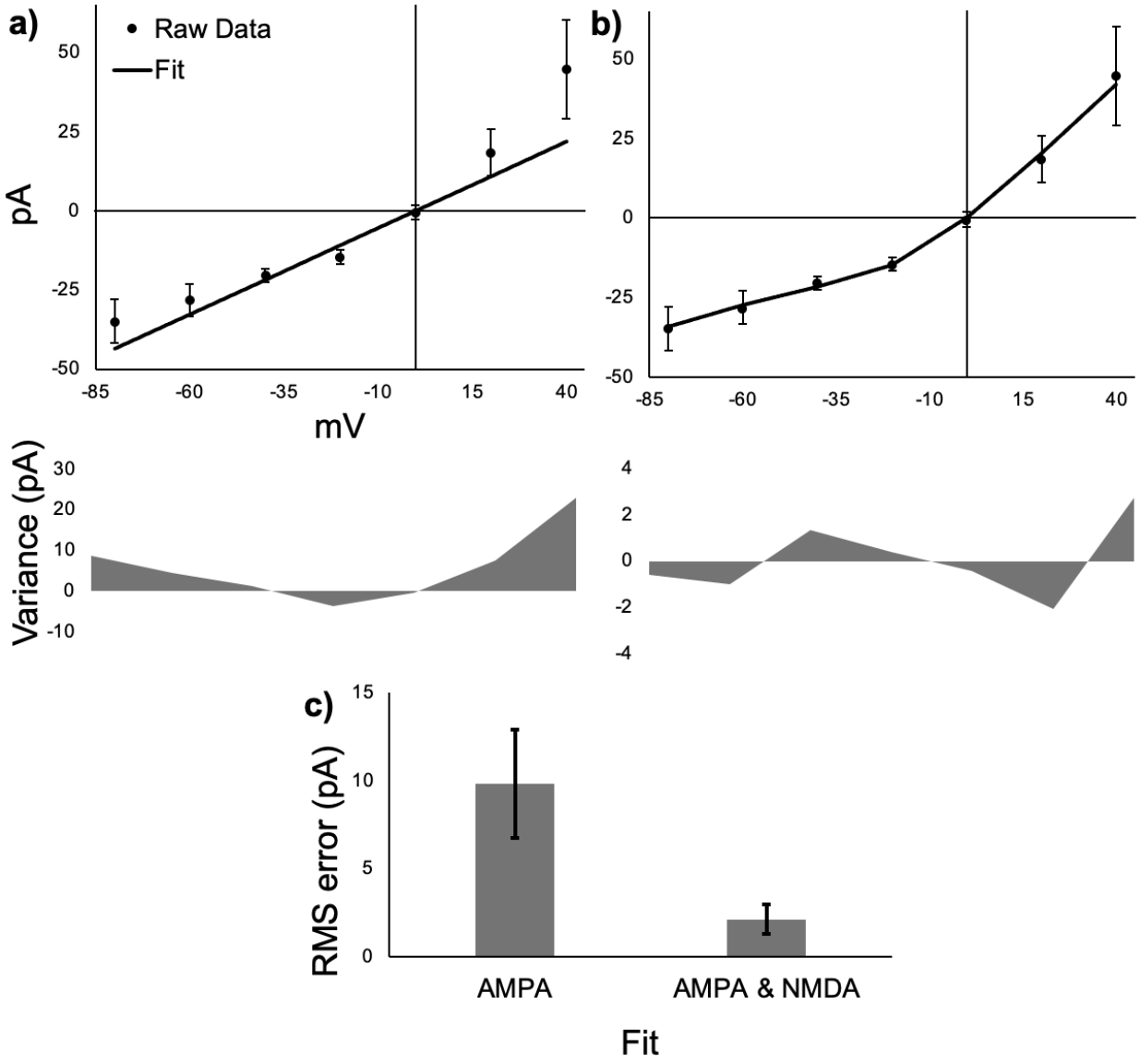

Figure 7. Comparison of fits using AMPAR alone vs combined AMPAR and NMDAR contributions to voltage-clamp electrophysiological recordings in mouse retina ON-GCs.

(a, top) shows the four-trial averaged experimental current-voltage relationship (raw data: black dots with SE bars) and fitted curve (solid black line) made using only the AMPAR basis function. (a, bottom) shows a graph of the variance between the experimental data and AMPAR-only fit. (b, top) depicts the same experimental data but fitted using a weighted sum of AMPAR and NMDAR basis functions. (b, bottom) indicates variance between the experimental data and the AMPAR/NMDAR fit. (c) compares the root mean square error between the experimental data and each fitted curve and error bars indicate SE

Chapter 3: Results

This section presents the results from my investigation into the contribution of NMDARs to contrast coding in ON-GCs of the mouse retina. I evaluated whether NMDARs contribute to low-contrast responses and how their contribution varies across the range of contrast levels. I determined individual receptor conductance values from whole-cell voltage clamp electrophysiological recordings using a mathematical deconvolution method.

3.1 NMDAR conductance in low contrast responses of ON-GCs

Previous research by Manookin et al., (2010) reported no contribution of NMDARs to low contrast responses in ON-$\propto$ GCs in guinea pigs. To explore whether this finding holds in mice ON-GCs, I investigated contributions to responses to low-contrast stimuli. I found that NMDARs had a relative contribution of 0.516 ± 0.0398 to the total low contrast conductance (Figure 8). The mean absolute NMDAR conductance was $0.788 \pm 0.299\ \mathrm{nS}$ (SE) with a median of 0.619 nS.

I assessed the distribution of NMDAR conductance values using the Shapiro-Wilk test, which indicated a significant deviation from normality ($W = 0.779$, $p = 0.038$). Based on this result, I used a one-tailed Wilcoxon signed-rank test to determine whether the median NMDAR conductance was significantly greater than zero. Results confirmed a significant contribution ($W = 21.0$, $p = 0.0156$).

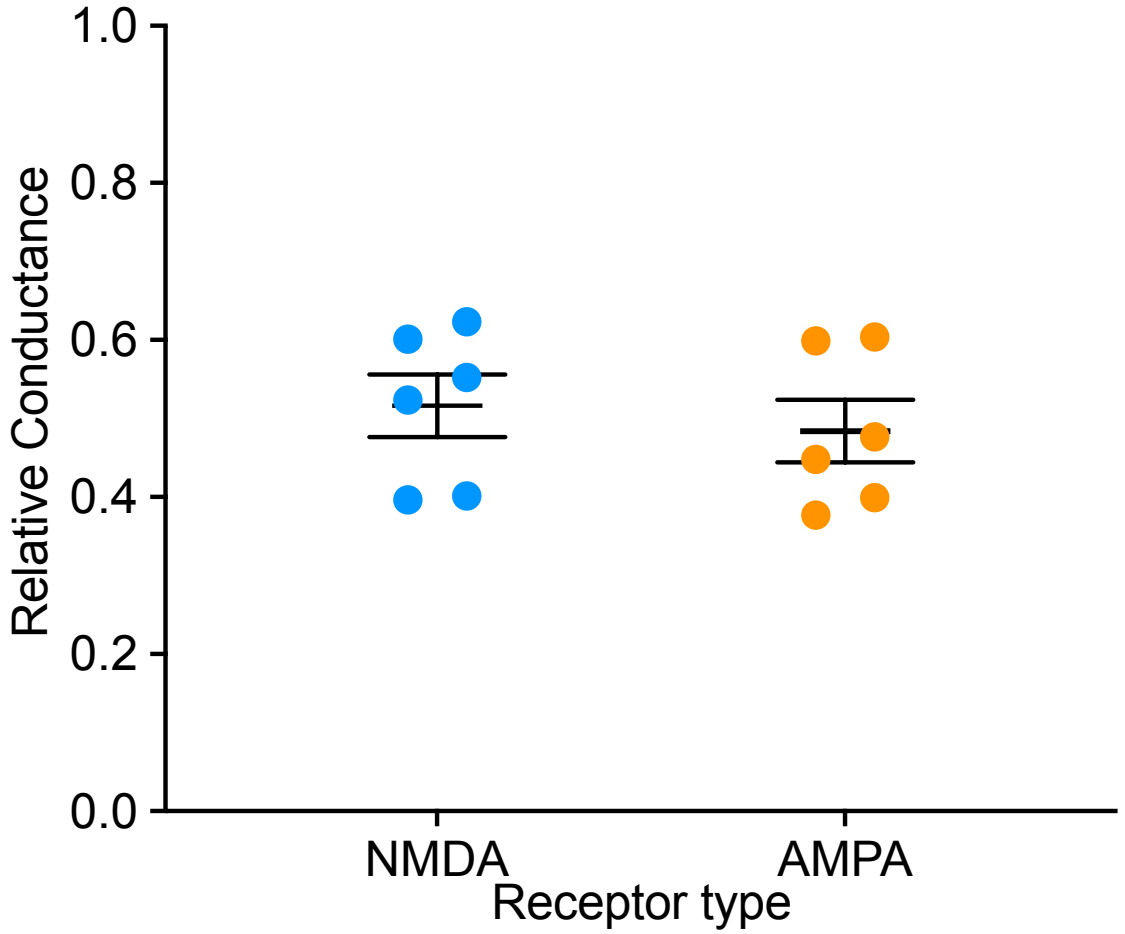

Figure 8. Relative conductance of AMPARs and NMDARs in response to low contrast stimuli in mice ON-GCs.

Grouped scatter plot showing the relative conductance of NMDARs (Blue) and AMPARs (Orange) in ON-GCs of the mouse retina in response to low-contrast light stimuli. Conductance is expressed as a fraction of the total conductance. Each data point represents an individual cell (n = 6); horizontal lines show the group means, and error bars represent the SEM. Conductance was determined mathematically from the current-voltage relationship of whole-cell voltage-clamp electrophysiological recordings.

3.2 NMDAR conductance across contrast levels in ON-GCs

Given Manookin et al., (2010) report of no NMDARs contribution at any contrast level in ON-$\propto$ GCs of guinea pigs, I investigated NMDAR conductance across contrast levels in ON-GCs of mice. I found that the mean NMDAR conductance increased with contrast: low (0.459 ± 0.150 nS), mid (0.992 ± 0.089 nS), and high (1.605 ± 0.077 nS) (Figure 9).

I used the Shapiro-Wilk test to assess the distribution of conductance values at each contrast level. The data met assumptions of normality: low (W = 0.827, p = 0.182), mid (W = 0.921, p = 0.455), and high (W = 0.818, p = 0.158). I then performed one-tailed, one-sample t-tests to determine whether the mean NMDAR conductance at each contrast level was significantly greater than zero: low (t = 3.05, p = 0.0463), mid (t = 11.2, p = 0.00395), and high (t = 20.9, p = 0.00115). Finally, I used one-tailed, paired-sample t-tests to assess whether NMDAR conductance increased with contrast. Conductance at high contrast was significantly greater than mid contrast (t = 21.09, p = 0.0011), and conductance at mid contrast was significantly greater than at low contrast (t = 3.72, p = 0.0327).

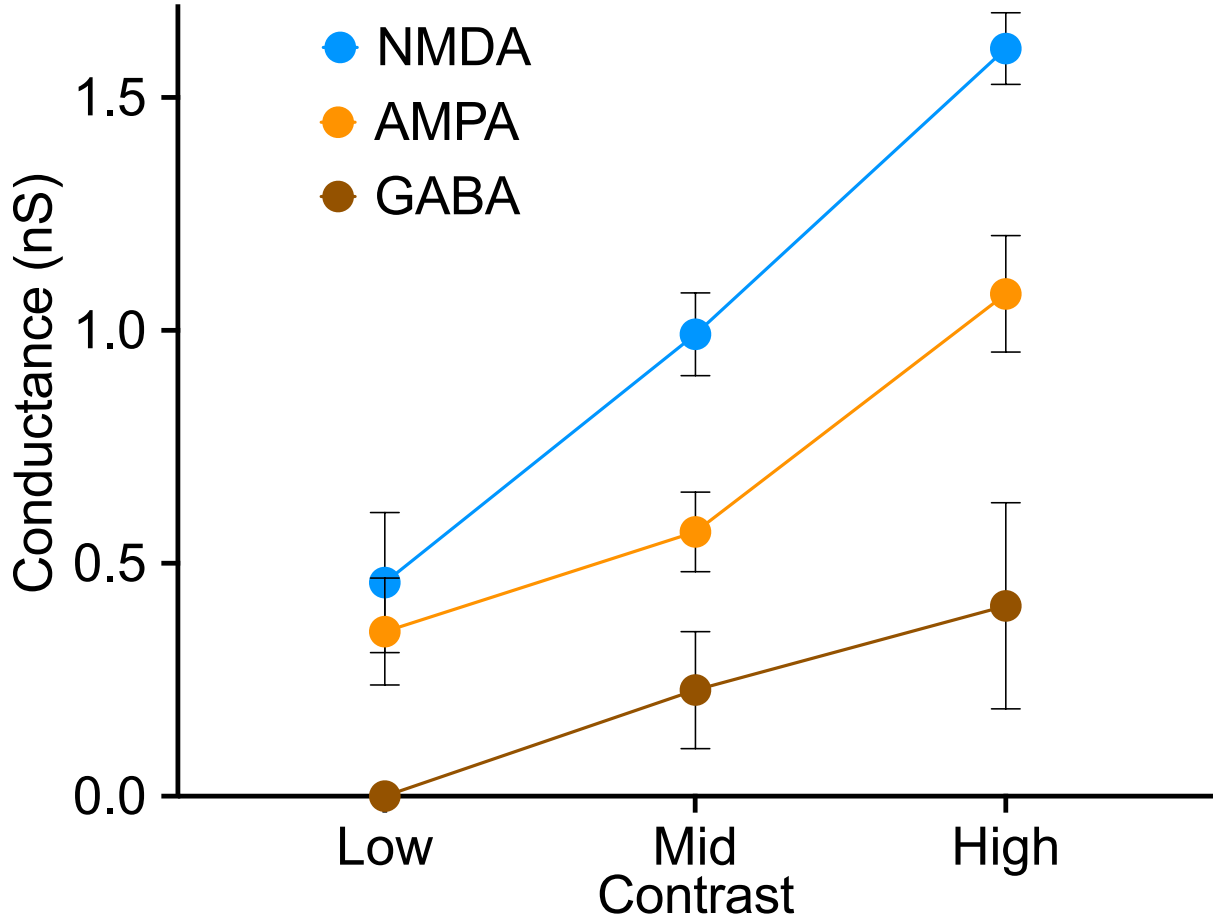

Figure 9. Conductance of NMDAR, AMPAR, and GABAR across contrast range in mice ON-GCs

A line graph showing the conductance of NMDARs, AMPARs, and GABARs in mouse ON-GCs of the retina across contrast levels. Data points represent the mean (n=3) conductance (nS), and error bars indicate the SEM. Colours correspond to receptor type: NMDA (blue), AMPA (orange), and GABA (brown). Conductance was determined mathematically from the current-voltage relationship of whole-cell voltage-clamp recordings.

Chapter 4: Discussion

The study aimed to investigate the contribution of NMDARs to contrast coding in mice ON-GCs. I particularly focusing on NMDARs role in encoding low contrast, as well as their involvement across varying contrast levels. The methods that I used included loose patch electrophysiology for cell identification and whole-cell voltage clamp electrophysiology for experimentation in combination with a mathematical deconvolution method. This approach using the deconvolution method allowed for quantification of NMDAR contributions without introducing potential non-specific pharmacological effects. My results showed that NMDARs contribute substantially to encoding low-contrast responses as well as across the entire contrast range by increasing with contrast.

4.1 NMDARs contribute to low-contrast responses.

The mean relative NMDAR conductance of 0.516 ± 0.0398 indicates a substantial role for NMDARs at low contrast. This contribution was statistically confirmed by demonstrating that the median conductance was significantly greater than zero (p=0.0156). Low contrast NMDAR mediated conductance has not been previously demonstrated in mice ON-GCs. Previous work by Manookin et al., (2010) reported no NMDAR contribution to low contrast responses in ON-$\propto$ GCs in guinea pigs. However, low contrast NMDAR contributions have been observed in other GC types in mice, such as direction selective GCs (Sethuramanujam et al., 2017). Overall, this finding shows NMDARs play a significant role in mediating low contrast responses in ON-GCs in mice. This extends our understanding of NMDARs diverse function in the retina and provides further insight into its roles in contrast coding across different cell types and species.

The observed contribution of NMDARs to low contrast responses prompts consideration of the potential underlying mechanisms. Low contrast stimulus would evoke low frequency glutamate release from BPCs which would likely be confined within the synaptic cleft. For this glutamate to bind NMDARs they would likely need to be synaptically localized. Therefore, the observed contributions of NMDARs contribution to low contrast may infer the presence of synaptically localized NMDARs receptors in ON-GCs.

4.2 NMDAR contribution to response across contrast levels by increasing in magnitude.

My results also showed a mean NMDAR conductance of 0.459 ± 0.150 nS at low contrast, 0.992 ± 0.089 nS at mid contrast, and 1.605 ± 0.077 nS at high contrast, indicating that NMDARs conductance is present at all contrasts and increases with contrast. I confirmed the presence of NMDARs at each contrast statistically by showing that conductance was significantly greater than zero (Low: p = 0.0463, Mid: p = 0.00395, high: p = 0.00115). I further confirmed the trend of increasing conductance, showing that at high contrast conductance was significantly greater than mid contrast (t = 21.09, p = 0.0011), and mid contrast was greater than low contrast (t = 3.72, p = 0.0327). NMDARs contributing to responses across the contrast range has not been previously documented in ON-GCs. It diverges from the results of Manookin et al., (2010) where NMDARs did not have any contribution at any contrast in guinea pig ON-$\propto$ GCs. Furthermore, contrast dependent scaling of NMDAR conductance has not been previously reported in ON-GCs. However, similar NMDAR scaling with stimulus strength has been documented in other parts of the nervous system, such as the visual cortex in cats (Fox & Daw 1990). Overall, these findings demonstrate that NMDARs contribute significantly to encoding the range of contrast by scaling in magnitude. This furthers our understanding in NMDARs roles in contrast coding and provides insight into ways that NMDARs can be utilized to encode stimulus in the retina. Furthermore, it shows mechanistic overlap to coding stimulus range with other areas of the nervous system.

The presence of NMDAR conductance across the contrast range prompts further speculation of receptor localization. I previously speculated that NMDARs could be localized synaptically in ON-GCs due to their contribution at low contrast. However, at high contrast levels when there is rapid glutamate release these receptors would likely saturate due to their high affinity. The continued NMDAR contribution at mid and high contrast suggests the presence of extrasynaptically localized receptors, which could be activated by glutamate spillover during high-frequency release. Therefore, the observed contrast-dependent scaling of NMDAR conductance may be mediated by widespread expression of NMDARs both synaptically and extrasynaptically. This provides grounds

for future research with more specific methodology to confirm receptor localization in these cells.

4.3 Limitations

Several limitations may have affected the results. First, interspecific variability in GC NMDAR expression may partly explain the discrepancies compared to other studies (Manookin et al., 2010). In addition, my study classified GCs solely based on electrophysiological criteria, lacking morphological or genetic analysis which is necessary for accurate determination of cell type (Sanes & Masland, 2015). Consequently, my results represent a broader, non-specific ON-GC population, which affects the comparability to other studies. Furthermore, the stimulus that was used may not have accurately represented the full contrast range. Ideally, the stimulus would be of many contrasts that start from zero gradually increasing to full contrast. However, the number of stimuli that could be presented at each voltage step was limited because clamping the cell for a long period at non-resting membrane potentials compromises the cell's viability. Lastly, the small sample size (although common in voltage-clamp electrophysiology) may limit the reliability of the results.

4.4 Future Research

The finding that NMDARs significantly contribute to responses at low contrast and across the contrast range in mouse ON-GCs lays the groundwork for several future investigations. A key direction involves replicating this experiment in clearly classified types of ON-GCs, to determine cell type-specific contributions of NMDARs to encoding contrast. Accurate classification could be achieved by using both electrophysiological and morphological identification. For the latter, a fluorescent dye could be added to the internal solution in the patch pipette during whole-cell recordings. This would allow for morphological analysis with fluorescence microscopy.

Further research should also focus on confirming the localization of NMDARs using pharmacological tools to clarify the underlying mechanisms that drive their involvement in contrast coding. Previous work has shown that NMDAR localization within GCs is dependent on subunit composition: receptors containing GluNR2A are

typically localized synaptically, whereas those containing GluNR2B are found extrasynaptically (Zhang & Diamond, 2009). Therefore, subunit-specific antagonists could be used to investigate the localization of contributing receptors. For instance, Ro 25-6981 could be used to selectively antagonist GluNR2B while MPX-004 could be used for GluNR2A. (Fischer et al., 1997; Volkmann et al., 2016). However, the use of pharmacology would potentially induce non-specific upstream effects on the retina, so the results would need to be interpreted carefully.

Finally, my study also highlights the broader application of the deconvolution method as a tool for investigating receptor specific conductances in electrophysiological recordings. However, further validation of this method is needed and could be achieved by testing its accuracy on mathematically modelled data.

4.5 Conclusion

This study demonstrated that NMDARs significantly contribute to contrast coding in mice ON-GCs, both at low contrast and across the range of contrasts. I quantified NMDAR conductances using whole-cell voltage clamp electrophysiology in addition to a mathematical deconvolution method. This deconvolution method allows for determination of receptor specific contributions without the use of pharmacology. I found that NMDARs play a substantial role encoding low contrast responses and scale with increasing contrast. These findings allow for speculation that NMDARs are localized both synaptically and extrasynaptically in ON-GCs in mice. These results diverge from previous literature investigating guinea pig ON-$\propto$ GCs which highlights interspecific and cell-specific differences in contrast coding mechanisms. This research extends our understanding of the diverse roles of NMDARs in the retina and suggests mechanisms that align with those observed in other parts of the nervous system. Together these findings provide new insights into the mechanisms of contrast coding in the retina and lay the groundwork for future research into cell-type specific NMDAR function and localization.

References

Baylor, D. A., & Fuortes, M. G. F. (1970). Electrical responses of single cones in the retina of the turtle*. The Journal of Physiology, 207*(1), 77–92. https://doi.org/10.1113/jphysiol.1970.sp009049

Berry, M. J., Warland, D. K., & Meister, M. (1997). The structure and precision of retinal spike trains. *Proceedings of the National Academy of Sciences*, *94*(10), 5411–5416. https://doi.org/10.1073/pnas.94.10.5411

Chen, S., & Diamond, J. S. (2002). Synaptically released glutamate activates extrasynaptic NMDA receptors on cells in the ganglion cell layer of rat retina. *The Journal of Neuroscience, 22*(6), 2165–2173. https://doi.org/10.1523/jneurosci.22-06-02165.2002

Connaughton, V. (1995). Glutamate and glutamate receptors in the vertebrate retina. In H. Kolb, E. Fernandez, B. Jones, & R. Nelson (Eds.), *Webvision: The organization of the retina and visual system.* University of Utah Health Sciences Center. http://www.ncbi.nlm.nih.gov/books/NBK11526/

Dingledine, R., Borges, K., Bowie, D., & Traynelis, S. F. (1999). The glutamate receptor ion channels*. Pharmacological Reviews, 51*(1), 7–61. https://doi.org/10.1016/S0031-6997(24)01394-2

Fischer, G., Mutel, V., Trube, G., Malherbe, P., Kew, J. N., Mohacsi, E., Heitz, M. P., & Kemp, J. A. (1997). Ro 25-6981, a highly potent and selective blocker of N-methyl-D-aspartate receptors containing the NR2B subunit. Characterization in vitro. *The Journal of pharmacology and experimental therapeutics, 283*(3), 1285–1292

Fox, K., Sato, H., & Daw, N. (1990). The effect of varying stimulus intensity on NMDA-receptor activity in cat visual cortex. *Journal of Neurophysiology, 64*(5), 1413–1428. https://doi.org/10.1152/jn.1990.64.5.1413

Ichinose, T., & Habib, S. (2022). On and off signaling pathways in the retina and the visual system. *Frontiers in Ophthalmology, 2*, 989002. https://doi.org/10.3389/fopht.2022.989002

Juusola, M., & French, A. S. (1997). The efficiency of sensory information coding by mechanoreceptor neurons. *Neuron, 18*(6), 959–968. https://doi.org/10.1016/s0896-6273(00)80335-9

Kalbaugh, T. L., Zhang, J., & Diamond, J. S. (2009). Coagonist release modulates NMDA receptor subtype contributions at synaptic inputs to retinal ganglion cells. *The Journal of Neuroscience, 29*(5), 1469–1479. https://doi.org/10.1523/jneurosci.4240-08.2009

Kaneko, A. (1970). Physiological and morphological identification of horizontal, bipolar and amacrine cells in goldfish retina. *The Journal of Physiology, 207*(3), 623–633. https://doi.org/10.1113/jphysiol.1970.sp009084

MacNeil, M. A., & Masland, R. H. (1998). Extreme diversity among amacrine cells: Implications for function. *Neuron, 20*(5), 971–982. https://doi.org/10.1016/s0896-6273(00)80478-x

Manookin, M. B., Weick, M., Stafford, B. K., & Demb, J. B. (2010). NMDA receptor contributions to visual contrast coding. *Neuron, 67*(2), 280–293. https://doi.org/10.1016/j.neuron.2010.06.020

Masland, R. H. (2012). The neuronal organization of the retina. *Neuron, 76*(2), 266–280. https://doi.org/10.1016/j.neuron.2012.10.002

Miller, R. F. (2008). Cell communication mechanisms in the vertebrate retina: The Proctor Lecture*. Investigative Ophthalmology & Visual Science, 49*(12), 5184–5198. https://doi.org/10.1167/iovs.08-2456

Molday, R. S., & Moritz, O. L. (2015). Photoreceptors at a glance. *Journal of Cell Science, 128*(22), 4039–4045. https://doi.org/10.1242/jcs.175687

Nowak, L., Bregestovski, P., Ascher, P., Herbet, A., & Prochiantz, A. (1984). Magnesium gates glutamate-activated channels in mouse central neurones. *Nature, 307*(5950), 462–465. https://doi.org/10.1038/307462a0

Patneau, D. K., & Mayer, M. L. (1990). Structure-activity relationships for amino acid transmitter candidates acting at N-methyl-D-aspartate and quisqualate receptors. *The Journal of Neuroscience, 10*(7), 2385–2399. https://doi.org/10.1523/JNEUROSCI.10-07-02385.1990

Purves, D., Augustine, G. J., Fitzpatrick, D., Katz, L. C., LaMantia, A.-S., McNamara, J. O., & Williams, S. M. (Eds.). (2001). *Neuroscience (2nd ed.). Sinauer Associates.* https://www.ncbi.nlm.nih.gov/books/NBK11107/

Sagdullaev, B. T., McCall, M. A., & Lukasiewicz, P. D. (2006). Presynaptic inhibition modulates spillover, creating distinct dynamic response ranges of sensory output. *Neuron, 50*(6), 923–935. https://doi.org/10.1016/j.neuron.2006.05.015

Sanes, J. R., & Masland, R. H. (2015). The types of retinal ganglion cells: Current status and implications for neuronal classification. *Annual Review of Neuroscience, 38*, 221–246. https://doi.org/10.1146/annurev-neuro-071714-034120

Sethuramanujam, S., Yao, X., Derosenroll, G., Briggman, K. L., Field, G. D., & Awatramani, G. B. (2017). “Silent” NMDA Synapses Enhance Motion Sensitivity in a Mature Retinal Circuit. *Neuron, 96*(5), 1099–1111.e3. https://doi.org/10.1016/j.neuron.2017.09.058

Shen, Y., Liu, X.-L., & Yang, X.-L. (2006). N-methyl-D-aspartate receptors in the retina. *Molecular Neurobiology, 34*(3), 163–179. https://doi.org/10.1385/MN:34:3:163

Singer, J. H. (2007). Multivesicular release and saturation of glutamatergic signalling at retinal ribbon synapses. *The Journal of Physiology, 580*(1), 23–29. https://doi.org/10.1113/jphysiol.2006.125302

Smirnakis, S. M., Berry, M. J., Warland, D. K., Bialek, W., & Meister, M. (1997). Adaptation of retinal processing to image contrast and spatial scale. *Nature, 386*(6620), 69–73. https://doi.org/10.1038/386069a0

Traynelis, S. F., Wollmuth, L. P., McBain, C. J., Menniti, F. S., Vance, K. M., Ogden, K. K., Hansen, K. B., Yuan, H., Myers, S. J., & Dingledine, R. (2010). Glutamate receptor ion channels: Structure, regulation, and function. *Pharmacological Reviews, 62*(3), 405–496. https://doi.org/10.1124/pr.109.002451

Volkmann, R. A., Fanger, C. M., Anderson, D. R., Sirivolu, V. R., Paschetto, K., Gordon, E., Virginio, C., Gleyzes, M., Buisson, B., Steidl, E., Mierau, S. B., Fagiolini, M., & Menniti, F. S. (2016). MPX-004 and MPX-007: New Pharmacological Tools to Study the Physiology of NMDA Receptors Containing the GluN2A Subunit. *PloS one, 11*(2), e0148129. https://doi.org/10.1371/journal.pone.0148129

Yedutenko, M., Howlett, M. H. C., & Kamermans, M. (2021). High Contrast Allows the Retina to Compute More Than Just Contrast. *Frontiers in Cellular Neuroscience, 14*. https://doi.org/10.3389/fncel.2020.595193

Zhang, J., & Diamond, J. S. (2009). Subunit- and pathway-specific localization of NMDA receptors and scaffolding proteins at ganglion cell synapses in rat retina. *The Journal of Neuroscience, 29*(13), 4274–4286. https://doi.org/10.1523/JNEUROSCI.5602-08.2009

Appendix

Appendix 1: Ringer's solution

110 mM NaCl, 2.5 mM KCl, 1 mM $CaCl_2$, 1.6 mM $MgCl_2$, 10 mM glucose, and 22 mM $NaHCO_3$).

Appendix 2: Internal solution

112.5mM CsCH3SO3, 8mM CsCl, 1mM MgCl2.6H2O, 1mM EGTA, 10mM HEPES, 2mM ATP.Mg2+ salt, 3mM QX314(Cl-) and 1mM GTP.Na3 salt) adjusted to 7.4 pH with CsOH.

Appendix 3: Calculating I-V point

$$\frac{\frac{\int_{t_1}^{t_2}(Current - baseline\ current)}{t_2 - t_1}}{Holding\ voltage}$$

Time intervals calculated from loose patch recording
t_1=Onset of spiking
t_2=Offset of spiking

Appendix 4: Fitting function

$$f(V) = a\left(e^{0.0105V} + 0.4602\right)(V + 56) + bV + \frac{cV}{1 + 0.213e^{-0.074V}}$$

a = GABA conductance

b = AMPA conductance

c = NMDA conductance